CO Reduction Mechanism

DOI: 10.1002/anie.201301470

Theoretical Considerations on the Electroreduction of CO to C_2 Species on Cu(100) Electrodes**

Federico Calle-Vallejo and Marc T. M. Koper*

The electroreduction of CO_2 or CO to hydrocarbons and other related compounds on Cu electrodes has attained remarkable interest since its discovery.[1] Most of the studies devoted to understanding its reaction mechanism have been experimental,[1e,f,2] while theoretical insight has been provided recently for the formation of C_1 species, such as CH_4, CO, and HCOOH.[3] This reaction offers the possibility of transforming carbon oxides into fuels for automotive applications (CH_4 and ethanol (EtOH)) and raw materials with wide and important industrial uses (C_2H_4). In the electrochemical environment of this reaction, that is, abundant protons and negative electrode polarization, diverse catalytic behaviors are observed: Ni, Fe, Pt, and Ti cathodes produce H_2 and no CO/CO_2 is reduced. Post-transition metals, such as Pb, In, Sn, and Tl mostly produce formate. Additionally, Au, Ag, Zn, and Pd reduce CO_2 only to CO. Cu has the exceptional ability to reduce CO_2/CO to CH_4, C_2H_4, EtOH, and a variety of other products.[1f,4] However, the large overpotentials hinder global spread of this technology.[1a] Thus, before any technical considerations on the implementation of electrolytic cells for CO_2/CO reduction are made, the fundamental problem of the electrocatalysis at the cathode must be solved. The first step towards an optimized performance is evidently the formulation of a mechanism able to explain the observed product distribution, the onset potentials, and the effect of different electrode facets and electrolyte concentrations on the catalytic activity. Herein we present a mechanism for the production of C_2H_4, EtOH, and acetaldehyde (MeCHO) from CO on Cu(100) electrodes. This facet has been reported to be particularly selective towards C_2H_4 production, with EtOH and MeCHO as C_2 side products.[1d] Another striking observation is that on Cu(100), C_2 products are formed at low overpotentials without the formation of C_1 products.[2b]

We will show that a mechanism that can explain the experimental observations on Cu(100) should have a rate-determining step (RDS) consisting of the coupling of two CO molecules mediated by electron transfer to form $*C_2O_2$. This dimer is transformed into C_2H_4 and EtOH by proton–electron transfer, according to the following overall reactions [Eq. (1) and (2)]:

$$2\,CO_{(g)} + 8(H^+ + e^-) \rightarrow C_2H_{4(g)} + 2\,H_2O_{(l)} \tag{1}$$

$$2\,CO_{(g)} + 8(H^+ + e^-) \rightarrow CH_3CH_2OH_{(l)} + H_2O_{(l)} \tag{2}$$

The adsorption energies, which include various corrections and appear in the Supporting Information, are calculated relative to CO (g) and ($H^+ + e^-$), using the Computational Hydrogen Electrode[5] (CHE) model in the way explained in the Supporting Information. The calculated onset potential of the reaction is the smallest applied potential U needed to make all steps exergonic, that is, the potential for which the free energies of all elementary reactions of a given pathway are negative or zero. The potential-determining step (PDS) of a given pathway is defined as the last step to become exergonic when the potential is modified.[3b,6] This model is purely thermodynamic and assumes that the kinetic barriers of uphill processes are not much larger than their reaction energies and that downhill processes have easily surmountable barriers.[3b] It has been shown theoretically that the barriers for proton transfer during the oxygen reduction can easily be overcome as they are approximately 0.15–0.25 eV,[7] and no double or triple bonds are entirely broken in a single step in the pathways found.

Figure 1 shows the lowest-overpotential pathways for the CO reduction to C_2H_4, MeCHO, and EtOH. Schematic representations of the intermediates are given in Figure 2. The energetic levels of all the species are given at $U = 0\ V_{RHE}$ (RHE = reversible hydrogen electrode) and at a calculated onset potential of $-0.40\ V_{RHE}$. This value is close to the one commonly accepted.[1a]

C–C bond lengths are useful to track the presence of multiple bonds in the intermediates. According to the energies provided in the Supporting Information, *COCHO, precursor of for example, glyoxal, is less stable than *CO-COH by 0.16 eV, suggesting a more favorable initial hydrogenation of the O atoms in $*C_2O_2$. *CO-COH has a C–C bond length of 1.46 Å, different from the values of 1.29 and 1.33 Å found in gas-phase for C_2O_2 and C_2H_4, indicating the existence of a single C–C bond. The alternatives for the hydrogenation of *CO-COH are *CCO + H_2O, precursor of C_2H_4, and *OHCCOH, *OHCCHO, and *OHCHCO, precursors of ethylene glycol and glycolaldehyde. We find that the route towards ethylene is thermodynamically favored by at least 0.75 eV. These results help explain why Kuhl et al.[1f] and Hori et al,[1a,e] found that the yields of all C_2 compounds other than ethanol and ethylene are below 1 % and have high onset potentials. Chemically speaking, the ease of protonation and subsequent dehydration of OH groups makes them more reactive in reducing environments than O atoms in carbonyl

---

[*] Dr. F. Calle-Vallejo, Prof. M. T. M. Koper
Leiden Institute of Chemistry, Leiden University
Einsteinweg 55, 2333 CC, Leiden (The Netherlands)
E-mail: m.koper@lic.leidenuniv.nl

[**] We acknowledge financial support from the NWO and the NRSC-C. The calculations were made in the NCF supercomputer facilities of the Netherlands.

Supporting information for this article is available on the WWW under http://dx.doi.org/10.1002/anie.201301470.

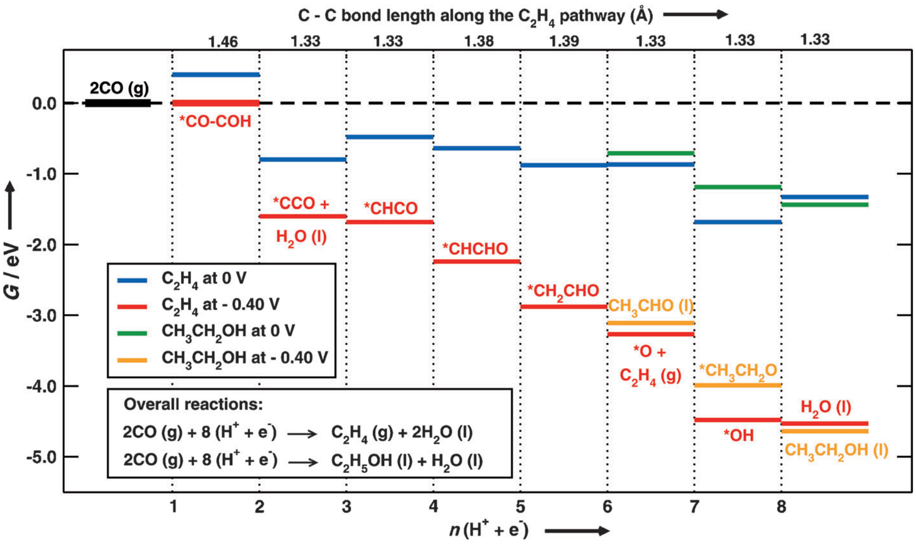

Figure 1. Lowest energy pathways for the electroreduction of CO to C_2H_4, MeCHO/EtOH at 0 V (blue, green) and −0.40 V (red, orange). The PDS is the first proton–electron transfer. C–C bond lengths are given in the upper *x*-axis for the pathway to C_2H_4.

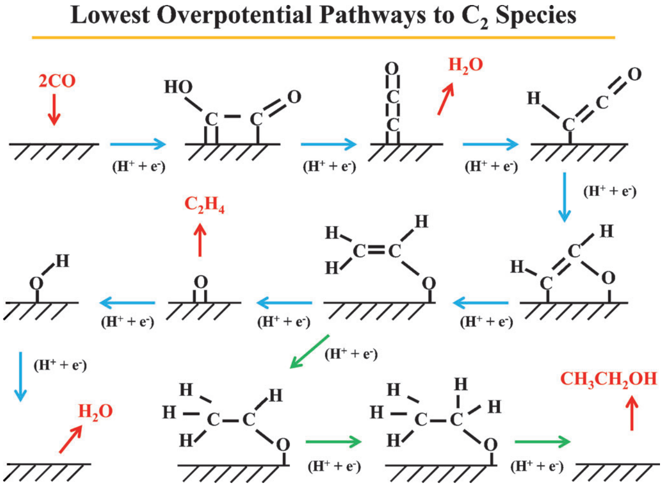

Figure 2. Schematic representations of the species involved in the pathways to C_2H_4 (blue) and MeCHO/EtOH (green).

groups, this being the reason why H_2O is desorbed in the next step leaving an adsorbed *CCO group.[8] *CCO has a C–C bond length of 1.33 Å, typical of C=C double bonds. From this point on, the subsequent proton–electron additions proceed such that the C–C double bond is preserved: the next step is an α-carbon protonation (*CHCO), followed by a protonation of the C atom in the carbonyl group (*CHCHO). This oxametallacycle binds to the surface through both C and O and has a C–C bond length of 1.39 Å. In the next step another protonation in the α-carbon takes place, producing $*CH_2CHO$. The next proton–electron transfer is rather important because in it the pathway to MeCHO/EtOH splits from that to C_2H_4 (See Figure 1 and 2). The C_2H_4 pathway proceeds with protonation of the C atom bonded to the O atom, resulting in the transient formation of $*CH_2CH_2O$. The C–O bond is rapidly cleaved and C_2H_4 is desorbed, leaving an *O adsorbate. *O is hydrogenated to *OH and then to H_2O. Alternatively, MeCHO is formed by protonation of the α-carbon in $*CH_2CHO$. Furthermore, MeCHO reduction to EtOH occurs via an ethoxy intermediate ($*CH_3CH_2O$). In case the thermodynamically unlikely hydrogenation of $*CH_2CHO$ to give vinyl alcohol (CH_2CHOH (g)) occurs, this unstable product would instantly tautomerize to MeCHO.[1f,9]

The fact that C_2H_4, MeCHO, and EtOH share the same pathway up to the fifth electrochemical step helps explaining some experimental features of the CO/CO_2 reduction. It is observed that C_2H_4 is the most abundant C_2 product (40.7% of current efficiency), followed by EtOH (12.8%) and MeCHO (1.0%) at a potential of $-1.39\ V_{SHE}$ (SHE = Standard hydrogen electrode).[1d] The proportion between EtOH and C_2H_4 can be rationalized qualitatively in terms of the favorability of the sixth hydrogenation step, which is inclined towards C_2H_4 formation by approximately 0.2 eV, but this should be corroborated by kinetic studies like those in Ref. [10]. The low yield of MeCHO is also the result of its further reduction to EtOH. It is important to consider the observations of Murata and Hori,[11] who found that the presence of different alkaline cations, that is, Li^+, Na^+, K^+, and Cs^+, affected the product selectivity of the CO/CO_2 reduction on Cu electrodes. Interestingly, they observed that these cations influenced the formation of C_2H_4 and EtOH in identical ways, indicating that they are formed in the same pathway. Recently, Kuhl et al.[1f] concluded that the presence of hydroxy and carbonyl groups in several C_2 and C_3 products of the CO_2 reduction is an indication of an early C–C coupling step, occurring before the cleavage of at least one of the C–O bonds in CO_2.

Another interesting experimental observation is that ethylene oxide (C_2H_4O) can be readily reduced to C_2H_4 at potentials lower than those required to reduce CO.[2a] The lowest-energy pathway for this reaction is given in Figure S5. The only uphill step is the clearance of *OH from the surface, which is predicted to start at −0.33 V. It can be inferred from Figure 1 and Figure S5 that adsorbed ethylene oxide ($*CH_2CH_2O$) is an intermediate of the reduction of both CO and C_2H_4O and that its dissociation into C_2H_4 (g) and *O is a thermodynamically favorable step, with a free energy change of approximately 0.4 eV. This situation confirms the conclusions of Schouten et al.,[2a] who suggested that adsorbed ethylene oxide might be a reaction intermediate of the CO reduction.

We draw our attention now to the first electrochemical step in Figure 1. The reaction is given in Equation (3).

$$* + 2\,CO_{(g)} + (H^+ + e^-) \rightarrow {}^*CO{-}COH \qquad (3)$$

In it, two CO molecules are coupled through their C atoms and one of the O atoms is hydrogenated. In the following, we will argue that Equation (3) is a reaction in which electron and proton transfer are effectively decoupled, and consists of three subsequent processes (see Figure 3 a): 1) CO adsorption; 2) coupling of *CO with CO(g) via electron transfer to form $^*C_2O_2^-$; 3) protonation of $^*C_2O_2^-$ to form *CO-COH. The reactions are given in Equations (4)–(6).

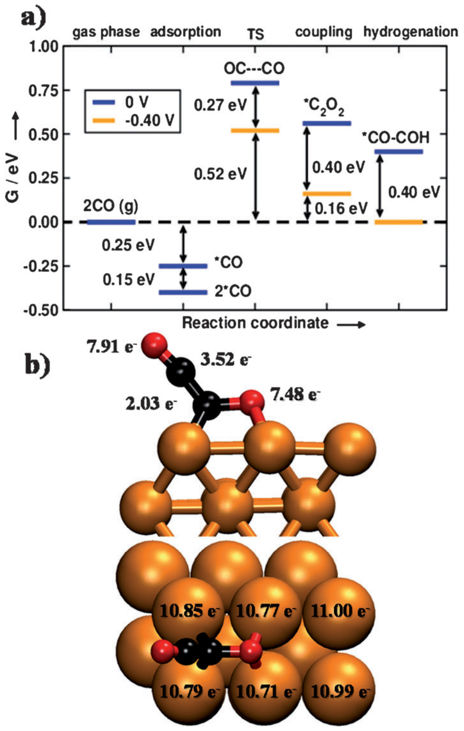

Figure 3. a) Deconvolution of the first electron–proton transfer at 0 V and −0.40 V. b) Adsorption geometry and Bader charges of the dimer and the surface. C black, O red.

$$* + CO_{(g)} \rightarrow {}^*CO \qquad (4)$$

$$^*CO + CO_{(g)} + e^- \rightarrow {}^*C_2O_2^- \qquad (5)$$

$$^*C_2O_2^- + H^+ \rightarrow {}^*CO{-}COH \qquad (6)$$

The CHE model predicts that at −0.40 V the overall reaction [Eq. (3)] will be thermodynamically feasible, provided that the reaction energies of uphill processes and barriers are similar, which is the case in Figure 3 a, where the free energies of $^*C_2O_2$ and its transition state and *CO-COH are close to each other at 0 V, within the accuracy of standard DFT. The decoupling of proton and electron transfer in Equation (3) explains a remarkable experimental observation of the CO reduction: while CH_4 formation depends on the pH value on the SHE scale, suggesting concerted proton–electron transfer, there is no influence of pH value on C_2H_4 formation on Cu(100).[1a,e,2a] This situation suggests that the rate-determining step happens at an early stage of the mechanism and that there should be no proton transfer involved in that step or in the ones before it.[2a] Thus, the only constraint in our search for the lowest-overpotential pathways was that C–C coupling should happen before the first proton transfer, and the fact that this step is found to be the PDS is purely an outcome of the calculations.

In favor of our hypothesis, we remark that in the general theory of proton-coupled electron transfer, such a decoupling will happen if the intermediate has a high electron affinity.[12] This is exactly the case for the dimer, as $C_2O_2^-$ and $C_2O_2^{2-}$ are more stable[13] than C_2O_2[14] (see also Figure S1), implying a favorable electron affinity of the dimer. Hori et al.[15] have argued that CO adsorption on Cu electrodes may be mediated by electron transfer, and did not observe this feature on other metals. Furthermore, in organic chemistry it is established that C–C coupling may occur through reductive CO coupling, in a reaction known as McMurry coupling, in which charged species or free radicals are involved.[8] From that perspective, after the electron transfer O acts as a strong nucleophile and reacts readily with H^+, forming an OH group and neutralizing the charge to form *CO-COH. Another argument in favor of the CO coupling under electrochemical conditions is found in experiments by Bard et al.,[16] who reduced CO in an aprotic solvent (liquid ammonia) to $C_2O_2^{2-}$ on Pt, Ni, C, and Hg electrodes at highly negative potentials. In the Supporting Information we show that while the calculated association enthalpy (ΔH) and its corresponding activation energy (E_a) for CO in gas phase to form C_2O_2 are high, 1.42 and 4.48 eV, the coupling through a charge-transfer mediated process to give $C_2O_2^-$ is evidently easier. Such process has a ΔH of −0.19 eV, implying a more favorable configuration of $C_2O_2^-$ (i.e. a favorable electron affinity) with respect to C_2O_2 and $E_a \approx 0.6$ eV, which is a reasonably surmountable barrier. Note that the addition of an electron decreases ΔH by approximately 1.5 eV and E_a by approximately 4 eV with respect to the charge-neutral situation.

Further support for our hypothesis is given in Figure 3 b. It contains the adsorption geometry of the most stable dimer found in our calculations and the corresponding Bader[17] charges of the surface atoms. $^*C_2O_2$ binds through both O and C to four Cu atoms. The number of valence electrons of the Cu atoms in the slab (and those in the layers below) which do not couple to the dimer is approximately 11, as expected. However, that number is approximately 10.75 for the other four Cu atoms, meaning that there is 1 e^- less at the surface. Conversely, the sum of the electrons of the dimer is approximately 21 e^-, one more than expected, as C has 4 valence electrons and O has 6. Hence, the dimer is negatively charged in its adsorbed state and we expect that it will be additionally stabilized by solvation effects (the extra charge on the dimer at the transition state is ca. 2/3 e^-, see the Supporting Information, which justifies the drop of 0.27 eV in the barrier at −0.40 V). The extra charge is located in the CO moiety that does not couple to the surface, which may allow further coupling to create the C_3 species observed by Kuhl et al.[1f] Note that the adsorption geometry in Figure 3 b would explain why Cu(100) is such an active surface for this reaction.[2b] Based on all the aforementioned observations, we propose the dimer formation on Cu(100) to occur by a sequential electron–proton transfer.

The mechanism with a rate-determining CO coupling step explains a number of experimental observations that other recent DFT-based models for C–C coupling in CO electroreduction cannot reproduce.[10,18] It naturally explains why on Cu(100) at low overpotential only C_2 products and not C_1 products are observed, whereas other models predict the simultaneous formation of CH_4 and C_2H_4. Secondly, the decoupling of proton–electron transfer in Equations (4)–(6), with the electron transfer being rate-determining, leads to a pH-independent C_2H_4 formation on the SHE scale, in agreement with experiments.[1a,e] This important experimental observation is not explained by other C–C coupling models, which assume concerted proton–electron transfers at every step in the mechanism and proceed by C–C coupling of hydrogenated C moieties. In the Supporting Information we briefly discuss the effect of H coadsorption and CO coverage on the results shown herein. We note that further studies are required to improve Cu electrodes by, for example, alloying, or to identify new materials capable of reducing CO_2/CO at low overpotentials.

Experimental Section

All DFT simulations were made with the VASP code.[19] Further details are given in the Supporting Information.

Received: February 19, 2013
Revised: April 16, 2013

Keywords: CO reduction · CO_2 reduction · density functional theory · electrocatalysis · reaction pathway

---

[1] a) M. Gattrell, N. Gupta, A. Co, *J. Electroanal. Chem.* **2006**, *594*, 1–19; b) Y. Hori, K. Kikuchi, A. Murata, S. Suzuki, *Chem. Lett.* **1986**, 897–898; c) Y. Hori, K. Kikuchi, S. Suzuki, *Chem. Lett.* **1985**, 1695–1698; d) Y. Hori, I. Takahashi, O. Koga, N. Hoshi, *J. Phys. Chem. B* **2002**, *106*, 15–17; e) Y. Hori, R. Takahashi, Y. Yoshinami, A. Murata, *J. Phys. Chem. B* **1997**, *101*, 7075–7081; f) K. P. Kuhl, E. R. Cave, D. N. Abram, T. F. Jaramillo, *Energy Environ. Sci.* **2012**, *5*, 7050–7059.

[2] a) K. J. P. Schouten, Y. Kwon, C. J. M. van der Ham, Z. Qin, M. T. M. Koper, *Chem. Sci.* **2011**, *2*, 1902–1909; b) K. J. P. Schouten, Z. Qin, E. P. Gallent, M. T. M. Koper, *J. Am. Chem. Soc.* **2012**, *134*, 9864–9867.

[3] a) W. J. Durand, A. A. Peterson, F. Studt, F. Abild-Pedersen, J. K. Norskov, *Surf. Sci.* **2011**, *605*, 1354–1359; b) A. A. Peterson, F. Abild-Pedersen, F. Studt, J. Rossmeisl, J. K. Norskov, *Energy Environ. Sci.* **2010**, *3*, 1311–1315; c) A. A. Peterson, J. K. Norskov, *J. Phys. Chem. Lett.* **2012**, *3*, 251–258.

[4] Y. Hori, H. Wakebe, T. Tsukamoto, O. Koga, *Electrochim. Acta* **1994**, *39*, 1833–1839.

[5] J. K. Nørskov, J. Rossmeisl, A. Logadottir, L. Lindqvist, J. R. Kitchin, T. Bligaard, H. Jónsson, *J. Phys. Chem. B* **2004**, *108*, 17886–17892.

[6] a) J. Rossmeisl, A. Logadottir, J. K. Norskov, *Chem. Phys.* **2005**, *319*, 178–184; b) I. C. Man, H.-Y. Su, F. Calle-Vallejo, H. A. Hansen, J. I. Martínez, N. G. Inoglu, J. Kitchin, T. F. Jaramillo, J. K. Nørskov, J. Rossmeisl, *ChemCatChem* **2011**, *3*, 1159–1165.

[7] V. Tripković, E. Skúlason, S. Siahrostami, J. K. Nørskov, J. Rossmeisl, *Electrochim. Acta* **2010**, *55*, 7975–7981.

[8] L. G. Wade, Jr., *Organic Chemistry*, 6th ed., Upper Saddle River, **2006**.

[9] R. P. Bell, M. H. Rand, K. M. A. Wynnejones, *Trans. Faraday Soc.* **1956**, *52*, 1093–1102.

[10] X. Nie, M. R. Esopi, M. J. Janik, A. Asthagiri, *Angew. Chem.* **2013**, *125*, 2519–2522; *Angew. Chem. Int. Ed.* **2013**, *52*, 2459–2462.

[11] A. Murata, Y. Hori, *Bull. Chem. Soc. Jpn.* **1991**, *64*, 123–127.

[12] M. T. M. Koper, *Phys. Chem. Chem. Phys.* **2013**, *15*, 1399–1407.

[13] a) J. R. Thomas, B. J. Deleeuw, P. Oleary, H. F. Schaefer, B. J. Duke, B. Oleary, *J. Chem. Phys.* **1995**, *102*, 6525–6536; b) W. E. Thompson, M. E. Jacox, *J. Chem. Phys.* **1991**, *95*, 735–745.

[14] a) N. H. F. Beebe, J. R. Sabin, *Chem. Phys. Lett.* **1974**, *24*, 389–394; b) D. Sülzle, T. Weiske, H. Schwarz, *Int. J. Mass Spectrom. Ion Processes* **1993**, *125*, 75–79; c) D. Talbi, G. S. Chandler, *J. Phys. Chem. A* **2000**, *104*, 5872–5881.

[15] Y. Hori, A. Murata, T. Tsukamoto, H. Wakebe, O. Koga, H. Yamazaki, *Electrochim. Acta* **1994**, *39*, 2495–2500.

[16] F. A. Uribe, P. R. Sharp, A. J. Bard, *J. Electroanal. Chem.* **1983**, *152*, 173–182.

[17] W. Tang, E. Sanville, G. Henkelman, *J. Phys. Condens. Matter* **2009**, *21*, 084204.

[18] J. H. Montoya, A. A. Peterson, J. K. Nørskov, *ChemCatChem* **2013**, *5*, 737–742.

[19] G. Kresse, J. Furthmuller, *Phys. Rev. B* **1996**, *54*, 11169–11186.